Effects of insert geometry and feed rate on quality characteristics of turned parts

M. N. Islam* and A. Pramanik

Department of Mechanical Engineering, Curtin University, Australia

Abstracts

This paper investigates experimentally and analytically the influence of insert geometry and feed rate on the quality characteristics of turned parts under the dry cutting condition. A three-level, three-parameter experiment was planned using the design of experiment methodology. The three levels of independent input parameters were: insert shape—rhombus, triangle, and square; nose radius 0.4, 0.8, and 1.2 mm; and feed rate—0.11, 0.22, and 0.33 mm/rev. The measured output parameters were the three most widely used quality characteristics of turned parts—diameter error, circularity, and surface finish (arithmetic average). The results were analyzed using three methods: traditional analysis, Pareto analysis of variation, and Taguchi method. The results reveal that two of the selected tool geometry parameters, insert shape and nose radius, influence diameter error considerably (total contribution 66.97%) and have minor effects on circularity (total contribution 3.67%) and surface finish (total contribution 11.60%). Feed rate is the major contributor to surface finish (76.42% contribution), whereas circularity is dominated by interaction effects such as insert shape–feed rate interaction (31.44% contribution).

Keywords *- Diameter error, circularity, surface roughness, Pareto ANOVA, Taguchi method*

*Corresponding author, Phone: +618 9266 3777, Fax: +618 9266 2681, Email: M.N.Islam@curtin.edu.au

1. INTRODUCTION

Machining operations are influenced by several input variables, of which the cutting tool used is the most critical [1]. The cutting tool affects almost all aspects of machining such as chip formation, heat generation, tool wear, dimensional accuracy, and surface finish. The influence of the cutting tool, especially its geometry, on the dimensional accuracy and surface finish of machined parts is clearer because the final shape, dimensions, finish, and special geometric details are generated through direct contact between the cutting tool and the workpiece. Feed rate is the other dominating factor that influences dimensional accuracy and surface finish because the feed rate regulates the frequency of workpiece–cutting tool contact.

Many researchers have investigated the effect of tool geometry and feed rate on various aspects of machining operations. Fang et al. [2] investigated the effects of chamfered and honed tools, covering a wide range of cutting speeds and feed rates, on three aluminum alloys: 7075-T6, 6061-T6, and 2024-T351. They concluded that the thrust force can be larger than the cutting force when the uncut chip thickness is less than a critical value, which varies with cutting speed and tool geometry for both chamfered and honed tools when rake angle becomes negative. The required cutting force increases, as cutting tool sharpness decreases.

Almeida et al. [3] noted that cutting force increases as the bluntness of the cutting edge increases in the following order: sharp > chamfer > hone. For the chemical vapor deposition (CVD) tool, chamfer preserves film integrity on the edge at feed rates below 0.06 mm/rev, whereas the film on a sharp-edged tool delaminates from the flank face during a machining test. Flank wear is always larger for chamfered tools than for sharp ones, while rake face wear is similar for both tool types under identical machining

conditions. Although cutting edge wear increases by aggravating the machining conditions, the integrity sharp-edged is better maintained.

Özel [4] observed that the effective rake angle is formed depending on the trapped workpiece material under the chamfer geometry, which affects cutting forces. Honed and chamfered cubic boron nitride (CBN) tools resulted in lower cutting forces but higher rake face temperatures. Chamfered CBN tools were found to result in lower rake face temperatures but the highest stresses in cutting and thrust directions.

Thiele et al. [5] noted the significance of edge geometry on surface roughness and cutting forces. Large edge hones result in higher average surface roughness values than do small edge hones owing to an increase in the extent of ploughing compared with shearing. The interaction of edge geometry and workpiece hardness affects surface roughness considerably. Additionally, large edge hones result in higher forces in the axial, radial, and tangential directions than do small edge hones. The effect of workpiece hardness on the axial and radial components of force is significant, particularly for large edge hones.

Hua et al. [6] found that the hone edge plus chamfer cutting edge and an aggressive feed rate help increase both compressive residual stress and penetration depth. Higher compressive residual stress in both the axial and circumferential directions of the machined surface can be obtained by choosing a higher feed rate, but doing so results in a significant increase in the cutting force. Increase in hone cutting edge radius facilitates the generation of compressive residual stress in the subsurface, but it leads to an increase in tool temperature as well. The effect of chamfer is equivalent to increasing hone radius. A medium hone radius (0.02–0.05 mm) combined with a chamfer angle of 20° are recommended. To obtain higher compressive residual stress while maintaining

low cutting force and cutting edge temperature, a small feed rate and high workpiece hardness are recommended. A medium hone radius plus chamfer in cutting edge preparation help lower tool temperature and cutting force.

The works described above have investigated the effect of cutting edge preparation and rake angle on machinability characteristics such as cutting force [7-8], residual stress [5, 9], chip formation [10, 11], heat generation [4, 11], and tool wear [12, 13]. A review of the effect of tool geometry on finish turning can be found in Dorga et al. [14]. Notably, not much information is available in the literature on the quality characteristics of machined parts. Furthermore, the absence of studies on the effect of insert shape, nose radius, and feed rate on dimensional accuracy in machining is noteworthy.

A number of studies [15-17] have discussed the dimensional accuracy and surface finish of turned parts, but they typically considered the effect of major cutting parameters—cutting speed, feed rate, and depth of cut. Others considered the effects of additional factors such as the cooling method [18-20], blank size [20], and work material [20]. Nevertheless, there is a lack of research on and understanding of (i) the effect of tool geometry (such as insert shape and nose radius) and feed rate and (ii) the interactions of these parameters on quality characteristics of machined parts, such as diameter error, circularity, and surface finish. To address this deficiency, in this study, we investigate the effects of insert shape, nose radius, and feed rate, as well as those arising from interaction among the aforementioned parameters, on the dimensional accuracy and surface finish of machined parts.

2. SCOPE

Single-point cutting tools used in turning operations are of three major types: (i) solid tool, (ii) brazed insert, and (iii) mechanically clamped insert. In current manufacturing practice, the mechanically clamped-type insert tool is the most popular choice as well as the topic of our investigation. Tool inserts are available in various shapes such as triangular, square, diamond, and circular. The cutting edge strength of an insert depends on its shape. The larger the nose angle, the higher is the edge strength. However, tools with larger nose angles require more power and exhibit a greater tendency to vibrate [21]. Therefore, the insert shape might influence the quality characteristics of finished parts, and it was thus selected as an input variable in this study.

Insert nose radius is another variable known to influence surface finish, chip breaking, and insert strength [22]. An increase in tool nose radius leads to an increase in thrust force. The thrust force:cutting force and thrust force:feed force ratios, too, increase with an increase in the tool nose radius. Residual stresses in the machined surface change from compressive to tensile as the nose radius increases [14]. Therefore, tool nose radius was selected as an input variable.

Feed rate, which is known to have a considerable influence on surface roughness, power requirement, and machining time, was selected as the third input variable. The following geometrical model is often used for calculating arithmetic average roughness (R_a) in turning operations [23]:

$$R_a = \frac{0.032\, f^2}{R} \tag{1}$$

where R is the tool nose radius in mm, and f is the feed rate in mm/rev.

Comparing the extents of the effects of insert geometry parameters with that of feed rate, one of the main cutting parameters, on the quality characteristics of finished parts is another reason for selecting feed rate alongside insert geometry parameters.

In the present study, the three most widely used quality characteristics of turned parts—diameter error, circularity, and surface finish—are selected. Diameter error, which represents size variation, is especially important for component parts involved in a cylindrical fit because the diameter error directly influences the clearance conditions of the fit. Circularity represents geometric variation, and it is significant for rotating component parts, where excessive circularity may cause unacceptable vibration and heat generation. A good surface finish is essential in a high quality part to prevent premature fatigue failure; improve corrosion resistance; reduce friction, wear and noise; and prolong product life. Surface finish can be expressed using a number of parameters such as the arithmetic average, root-mean-square roughness, peak-to-valley height, and ten-point height. Given its simplicity, arithmetic average is the most commonly used roughness parameter. As such, we adopted arithmetic average to represent surface roughness.

This study investigates effect of individual input parameters as well as their interactions.

The results were analyzed by applying three techniques—traditional analysis, Pareto analysis of variation (ANOVA), and Taguchi's signal-to-noise (S/N). Traditional analysis employs the mean values of the responses, and it is primarily used for expressing relationships between input and output variables. However, the method does not provide a complete picture because it does not typically include data on variation of the responses.

Pareto ANOVA is an excellent tool for determining the contribution of each input parameter and its interactions with other input parameters on the output parameters. It is a simplified ANOVA analysis method that does not require either an ANOVA table or *F*-tests. Therefore, it does not require detailed knowledge about the ANOVA method. Details on Pareto ANOVA are available in the literature [24].

The Taguchi method is another popular tool for parameter design. It applies signal-to-noise (S/N) ratio as a quantitative analysis tool for optimizing the outcome of a manufacturing process. The S/N ratio can be calculated using the following formula [25]:

$$S/N = -10\log\frac{1}{n}\left(\sum_{i=1}^{n} y_i^2\right) \tag{2}$$

where *n* denotes number of observations, and *y* denotes observed data.

The above formula is suited to those quality characteristics for which the adage “the smaller the better” holds. All the three quality characteristics considered herein fall in this category. The higher the S/N ratio, the better is the result, because a high S/N ratio guarantees the highest quality with minimum variance. A thorough treatment of the Taguchi method can be found in [25].

3. EXPERIMENTAL WORK

In this study, insert shape, nose radius, and feed rate were varied during the turning of AISI-4340 steel, while maintaining the other variables constant. These variables were maintained at the three levels listed in Table 1. Preferably, insert nose angle should be selected as the control variable rather than insert shape because nose angle has a more

direct relationship with the quality characteristics of a part. However, we selected insert shape instead to represent the discrete nature of the variable.

Table 1: Input parameters

Input parameters	Unit	Symbol	Levels		
			Level 0	Level 1	Level 2
Insert shape		A	 Rhombus	 Triangle	 Square
Nose radius	mm	B	0.4	0.8	1.2
Feed rate	mm/rev	C	0.11	0.22	0.33

Developing an experiment involving variable insert parameters by using the design of experiment method is challenging because the method requires changing one variable at a time while keeping all other variables unchanged. It is difficult to obtain the appropriate combinations. In insert nomenclature [26], four letters are used. The first letter represents the shape of the insert, while the second, third, and fourth letters represent clearance angle, tolerance class, and geometry (feature), respectively. Nine coated carbide inserts were used with combinations of three insert shapes (DNMG, TNMG, and CNMG) and three nose radii (see Table 1), while maintaining all remaining variables, such as clearance angle and insert tolerance, at their respective values. DNMG and CNMG inserts are rhombus-shaped with nose radii of 55º and 80º, respectively, whereas TNMG inserts are triangular with a 60º nose radius. Thus, technically, CNMG is not square-shaped, but here it is described as square-shaped for convenience.

The experiments were planned using Taguchi's orthogonal array. A three-level, three-parameter L_{27} orthogonal array [27] was selected for our experiments. The details of input parameter combinations are summarized in Table 2. A total of 27 experimental runs were conducted in nine parts, each of which was divided into three segments, and

the experiments were performed according to the design of experiment. Each part was turned with a new insert to avoid any effect of tool wear. The inserts were manufactured by Stellram (USA). The chemical composition of the work material (AISI-4340 steel), compiled from Matweb [28], is listed in Table 3. The nominal dimensions of each part were length = 170 mm length and diameter = 40 mm. The experiment was carried out on a Harrison conventional lathe with a 330 mm swing under the dry condition. The depth of cut (1 mm) and cutting speed (212 m/min) were maintained constant. The diameter error and circularity were measured using a Discovery Model D-8 coordinate measuring machine (CMM), manufactured by Sheffield (UK). The surface roughness parameter, arithmetic average (R_a), for each turned surface was measured using a Surftest SJ-201P, manufactured by Mitutoyo (Japan).

Table 2: Array of machining parameters used in this work [27]

	Column Number												
Experiment	A	B	AxB	AxB	C	AxC	AxC	BxC	-	-	BxC	-	-
No	1	2	3	4	5	6	7	8	9	10	11	12	13
1	0	0	0	0	0	0	0	0	0	0	0	0	0
2	0	0	0	0	1	1	1	1	1	1	1	1	1
3	0	0	0	0	2	2	2	2	2	2	2	2	2
4	0	1	1	1	0	0	0	1	1	1	2	2	2
5	0	1	1	1	1	1	1	2	2	2	0	0	0
6	0	1	1	1	2	2	2	0	0	0	1	1	1
7	0	2	2	2	0	0	0	2	2	2	1	1	1
8	0	2	2	2	1	1	1	0	0	0	2	2	2
9	0	2	2	2	2	2	2	1	1	1	0	0	0
10	1	0	1	2	0	1	2	0	1	2	0	1	2
11	1	0	1	2	1	2	0	1	2	0	1	2	0
12	1	0	1	2	2	0	1	2	0	1	2	0	1
13	1	1	2	0	0	1	2	1	2	0	2	0	1
14	1	1	2	0	1	2	0	2	0	1	0	1	2
15	1	1	2	0	2	0	1	0	1	2	1	2	0
16	1	2	0	1	0	1	2	2	0	1	1	2	0
17	1	2	0	1	1	2	0	0	1	2	2	0	1
18	1	2	0	1	2	0	1	1	2	0	0	1	2
19	2	0	2	1	0	2	1	0	2	1	0	2	1
20	2	0	2	1	1	0	2	1	0	2	1	0	2
21	2	0	2	1	2	1	0	2	1	0	2	1	0
22	2	1	0	2	0	2	1	1	0	2	2	1	0
23	2	1	0	2	1	0	2	2	1	0	0	2	1
24	2	1	0	2	2	1	0	0	2	1	1	0	2
25	2	2	1	0	0	2	1	2	1	0	1	0	2
26	2	2	1	0	1	0	2	0	2	1	2	1	0
27	2	2	1	0	2	1	0	1	0	2	0	2	1

Table 3: Chemical composition of work material (AISI-4340 steel) [28]

Carbon, C	0.370 – 0.430 %
Chromium, Cr	0.700 – 0.900 %
Iron, Fe	95.195 – 96.33 %
Manganese, Mn	0.600 – 0.800 %
Molybdenum, Mo	0.200 – 0.300 %
Nickel, Ni	1.65 – 2.00 %
Phosphorus, P	≤ 0.0350 %
Silicon, Si	0.1500 – 300 %
Sulphur, S	≤ 0.0400%

4. RESULTS AND ANALYSIS

The experimental results for diameter error, circularity, and surface roughness, as well as their corresponding S/N ratios, are summarized in Table 4. Analyses of the results, performed using Pareto ANOVA, the Taguchi method, and traditional analysis, are presented in subsequent subsections.

Table 4: Experimental results for diameter error, circularity, and surface roughness, and their corresponding S/N ratios

Experiment number	Measured Parameters			Calculated S/N ratio		
	Diameter error (mm)	Circularity (μm)	Surface roughness (μm)	S/N ratio for diameter error	S/N ratio for circularity	S/N ratio for surface roughness
1	0.20	9.00	1.08	14.20	-20.40	-0.72
2	0.23	8.33	3.57	12.69	-18.51	-11.06
3	0.23	5.67	8.56	12.94	-15.10	-18.67
4	0.26	8.67	0.48	11.78	-19.07	6.38
5	0.28	3.67	2.26	11.11	-11.36	-7.08
6	0.29	6.33	4.27	10.79	-16.13	-12.61
7	0.20	5.00	0.67	13.99	-13.98	3.46
8	0.14	6.00	2.30	17.01	-15.80	-7.24
9	0.20	8.67	4.60	13.81	-20.11	-13.26
10	0.18	6.67	1.09	15.07	-16.50	-0.78
11	0.19	6.33	4.46	14.47	-16.13	-12.98
12	0.18	5.67	10.53	15.09	-15.27	-20.49
13	0.27	8.33	0.56	11.53	-19.40	5.11
14	0.26	7.67	1.16	11.86	-19.46	-1.26
15	0.21	5.00	5.14	13.60	-14.09	-14.22
16	0.20	4.33	0.37	13.91	-12.79	8.51
17	0.23	12.00	1.30	12.63	-22.70	-2.28
18	0.20	9.00	2.71	13.84	-19.12	-8.65
19	0.24	7.00	1.02	12.56	-17.08	-0.22
20	0.23	5.00	0.81	12.83	-14.09	1.78
21	0.28	7.33	2.30	11.20	-17.78	-7.25
22	0.25	6.00	0.70	11.97	-15.56	3.07
23	0.38	4.67	1.56	8.31	-13.42	-3.93
24	0.39	7.00	3.34	8.23	-17.30	-10.48
25	0.20	4.00	0.45	14.07	-12.22	6.89
26	0.18	4.33	1.89	15.09	-12.79	-5.52
27	0.25	21.00	3.17	11.82	-28.03	-10.03

4.1 Diameter Error

The Pareto ANOVA analysis for diameter error is summarized in Table 5. It shows that the nose radius (B) has the most significant effect on diameter error, with a contribution ratio P ≅ 50%, followed by insert shape (A) (P ≅ 17%). The interaction between insert shape and feed rate (A × C) and that between insert shape and nose radius (A × B) played roles as well, with contributions of 8.7% and 8.4%, respectively. Feed rate (C) showed a small effect (P ≅ 4%). It is worth pointing out that the total contribution of the main effects was about 71% and that of the interaction effects was about 29%. Consequently, it is moderately difficult to optimize diameter error by selecting input parameters.

Table 5: Pareto ANOVA analysis for diameter error

Sum at factor level	Factor and interaction								
	A	B	AxB	AxB	C	AxC	AxC	BxC	BxC
0	118.32	121.05	108.71	117.79	119.08	118.71	110.17	119.18	112.56
1	121.99	99.17	119.28	110.64	115.99	112.58	121.93	114.73	114.57
2	106.07	126.16	118.39	117.95	111.31	115.09	114.28	112.47	119.24
Sum of squares of difference (S)	416.89	1233.05	206.25	104.38	91.71	56.96	213.76	70.01	70.46
Contribution ratio (%)	16.92	50.05	8.37	4.24	3.72	2.31	8.68	2.84	2.86
	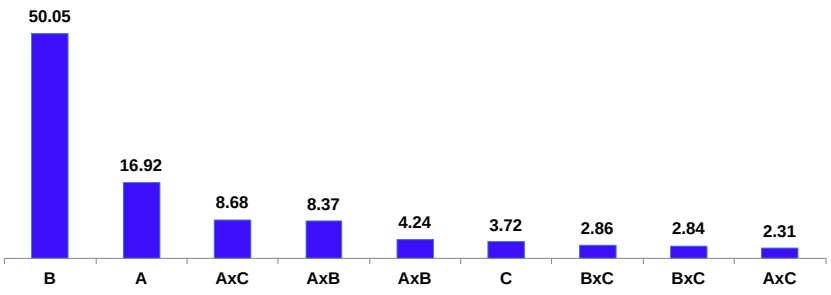								
Cumulative contribution	50.05	66.98	75.65	84.03	88.26	91.99	94.85	97.69	100.00
Check on significant interaction			AXC two-way table						
Optimum combination of significant factor level			A1B2C0						

The response table and response graphs of the mean S/N ratio are presented in Table 6 and shown in Fig. 1, respectively. These results confirm the findings of the Pareto ANOVA analysis, summarized in Table 5. The results show that parameter B (nose radius) has the most significant effect on diameter error (see Max-Min column in Table 6), and its high level (B2) provides the lowest diameter error (Fig. 1). Because the

interaction A × C was significant, an A × C two-way table was constructed for selecting their levels. The two-way tables are not included in this paper owing to space constraints. The two-way table of A × C interactions showed that A1C0 yielded the lowest diameter error. Therefore, the best combination of input parameters for achieving the best diameter error is A1B2C0, i.e., when the insert shape is triangular (nose angle = 60°), nose radius is 1.2 mm, and feed rate is 0.11 mm/rev.

Table 6: Response table for mean S/N ratio for diameter error, and significant interaction

		Mean S/N Ratio			
Input Parameters	**Symbol**	**Level 0**	**Level 1**	**Level 2**	**Max - Min**
Insert Shape	A	13.15	13.55	11.79	1.77
Noise Radius	B	13.45	11.02	14.02	3.00
Feed Rate	C	13.23	12.89	12.37	0.86
Interaction A×C	A×C	12.24	13.55	12.70	1.31

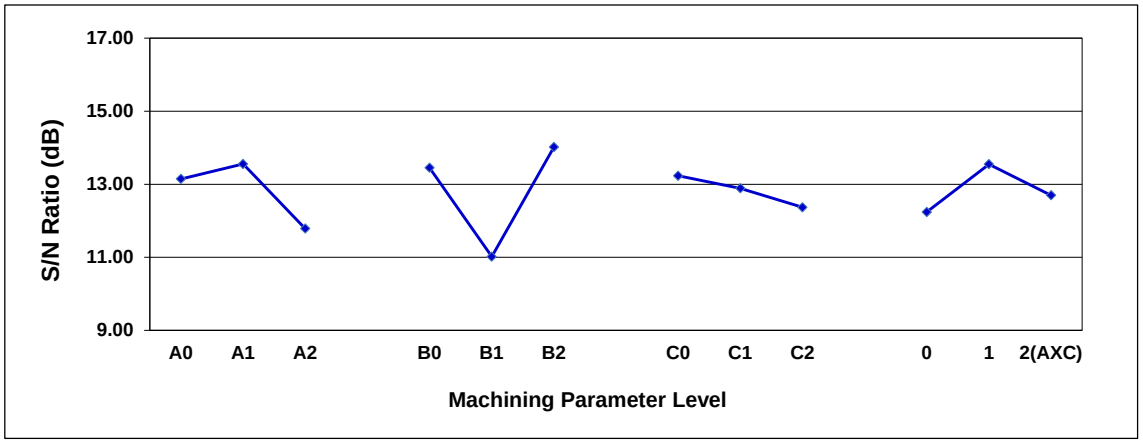

Fig. 1 Response graphs of mean and S/N ratio for diameter error

The results of traditional analyses, showing the average variation of diameter error for three input parameters, are presented in Fig. 2. The dominant effect of nose radius is evident from this figure. Moreover, the figure shows that the minimum diameter error is achieved at the mid level of insert shape (nose angle of 60°), high level of nose radius

(1.2 mm), and low level of feed rate (0.11 mm/rev). These findings confirm those obtained from the Pareto ANOVA analysis, summarized in Table 5, and Taguchi method, summarized in Table 6 and shown in Fig. 1.

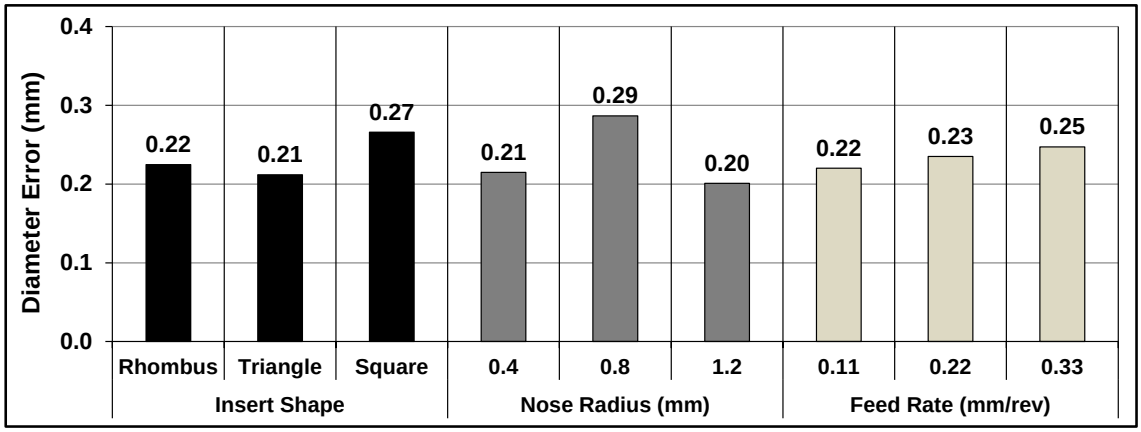

Fig. 2 Average variation of diameter error for three input parameters

4.2 Circularity

The Pareto ANOVA analysis for circularity is summarized in Table 7. In this Pareto analysis, dominance of the interaction effects is noteworthy. The interaction between insert shape and feed rate (A × C) has the highest influence (P ≅ 31%), followed by the interaction effects of nose radius and feed rate (B × C) (P ≅ 28% and 18%). Among the individual variables, feed rate (C) has the most significant effect on circularity, with a contribution ratio P ≅ 8%, followed by nose radius (B) (P ≅ 3%), and insert shape (A) (P ≅ 1%). The total contribution of the interaction effects is about 89%, whereas that of the main effects is 11%, thus making it highly difficult to optimize the circularity error by selecting suitable input parameters.

Table 7: Pareto ANOVA analysis for circularity

Sum at factor level	Factor and interaction								
	A	B	AxB	AxB	C	AxC	AxC	BxC	BxC
0	-150.45	-150.86	-154.90	-160.00	-146.99	-142.24	-174.84	-152.78	-165.49
1	-155.45	-145.79	-147.49	-150.11	-144.26	-157.46	-139.01	-170.03	-135.24
2	-148.27	-157.53	-151.79	-144.08	-162.94	-154.48	-140.33	-131.38	-153.46
Sum of squares of difference (S)	81.29	208.27	83.03	387.76	610.72	390.44	2476.97	2249.19	1391.49
Contribution ratio (%)	1.03	2.64	1.05	4.92	7.75	4.96	31.44	28.55	17.66
	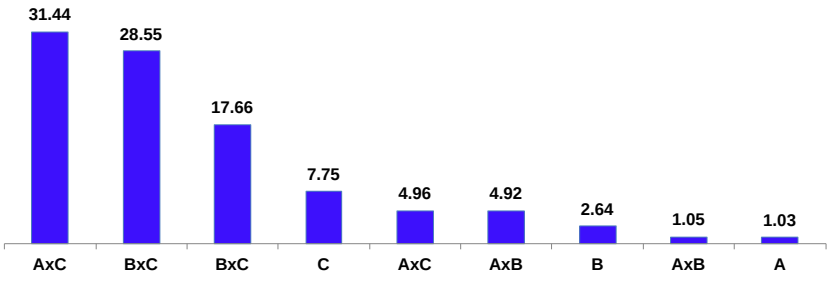								
Cumulative contribution	31.44	59.98	77.64	85.39	90.35	95.27	97.91	98.97	100.00
Check on significant interaction			AXC two-way table						
Optimum combination of significant factor level			A0B1C1						

The response table and the response graphs of the mean S/N ratio are presented in Table 8 and shown in Fig. 3, respectively. The results confirm the findings of the Pareto ANOVA analysis given in Table 7. The results show that parameter A × C (interaction between nose radius and feed rate) has the most significant effect on circularity. Compared with other variables, the effect of insert shape (A) is negligible. A two-way table of A × C interactions showed that A0C1 achieved the best circularity, that is, a rhombus-shaped insert and a feed rate of 0.22 mm/rev. Table 8 and Figure 3 show that the best level for parameter B is the mid level (B1) Therefore, the combination of input variables that yields the least circularity error is A0B1C1 i.e., rhombus-shaped insert (nose angle of 55°), mid level of nose radius (0.8 mm), and mid level of feed rate (0.22 mm/rev).

Table 8: Response table for mean S/N ratio of circularity, and significant interaction

		Mean S/N Ratio			
Input Parameters	**Symbol**	**Level 0**	**Level 1**	**Level 2**	**Max - Min**
Insert Shape	A	-16.72	-17.27	-16.47	0.80
Noise Radius	B	-16.76	-16.20	-17.50	1.31
Feed Rate	C	-16.33	-16.03	-18.10	2.08
Interaction A×C	A×C	-19.43	-15.45	-15.59	3.98

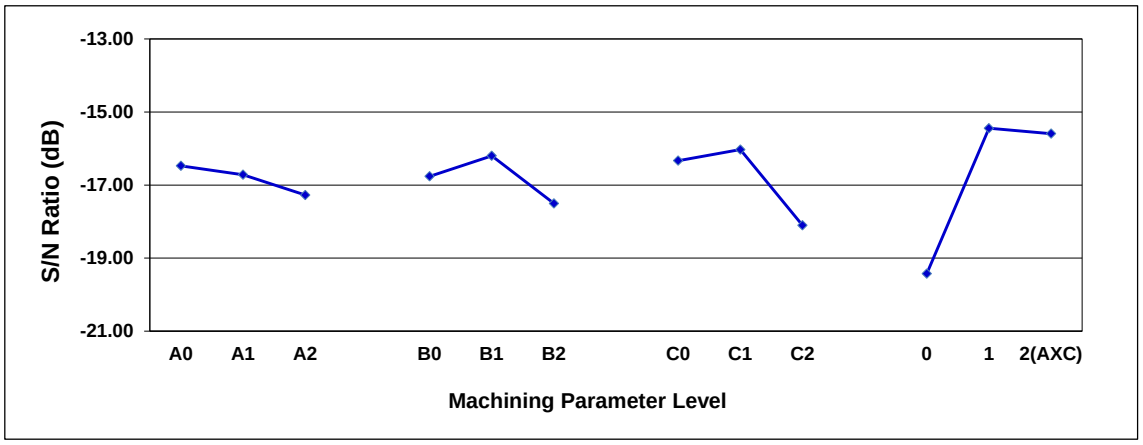

Fig. 3 Response graphs of mean and S/N ratio for circularity

The results of traditional analyses, which present the averaged variation of circularity for three input parameters, are shown in Fig. 4. Compared with those of the other input parameters, the influence of insert shape on circularity is very small. Moreover, the best circularity is achieved at the low level of insert shape i.e., rhombus-shaped insert (nose angle of 55°), and the mid levels of nose radius (0.8 mm) and feed rate (0.22 mm/rev). These findings agree with those of the Pareto ANOVA analysis, summarized in Table 7, and the Taguchi method, summarized in Table 8 and shown in Fig. 3.

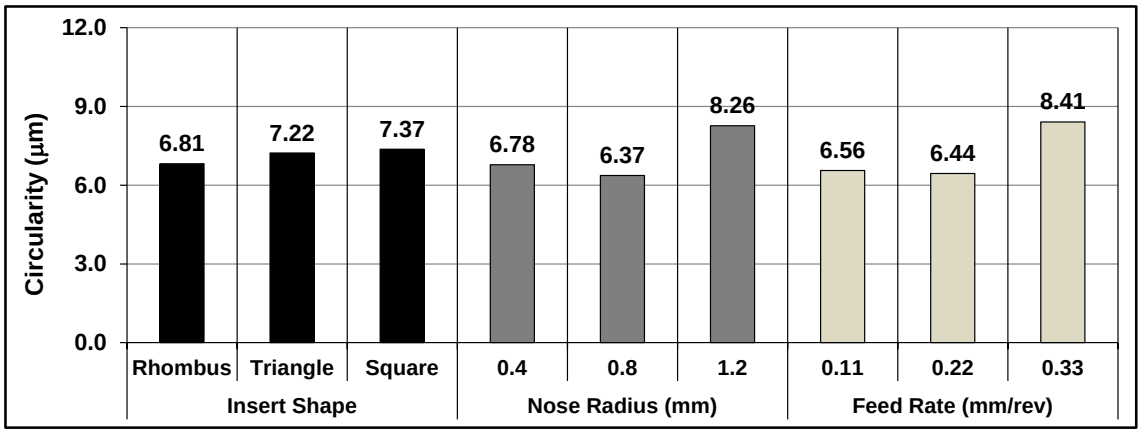

Fig. 4 Average variation of circularity for three input parameters

4.3 Surface Roughness

The Pareto ANOVA analysis for surface roughness is summarized in Table 9. Feed (C) has the most significant effect on surface roughness (P ≅ 76%), followed by nose radius (B) (P ≅ 7%). The interactions between insert shape and nose radius (A × B), too, played a role, with a contribution of P ≅ 6%. Insert shape (A) showed a small effect (P ≅ 4%). The total contribution of the main effects is about 88% and that of the interaction effects of is about 12%. Therefore, it is relatively easy to optimize surface finish by selecting the input parameters, especially through proper feed rate selection.

Table 9: Pareto ANOVA analysis for surface roughness

Sum at factor level	Factor and interaction								
	A	B	AxB	AxB	C	AxC	AxC	BxC	BxC
0	-60.79	-70.38	-44.21	-49.47	31.70	-41.89	-35.14	-54.07	-45.93
1	-47.03	-35.02	-56.20	-21.41	-49.57	-40.29	-59.00	-39.62	-40.71
2	-25.69	-28.10	-33.10	-62.62	-115.65	-51.32	-39.36	-39.82	-46.87
Sum of squares of difference (S)	1876.56	3085.53	801.30	2658.61	32683.30	213.12	972.54	411.58	66.18
Contribution ratio (%)	4.39	7.21	1.87	6.22	76.42	0.50	2.27	0.96	0.15
	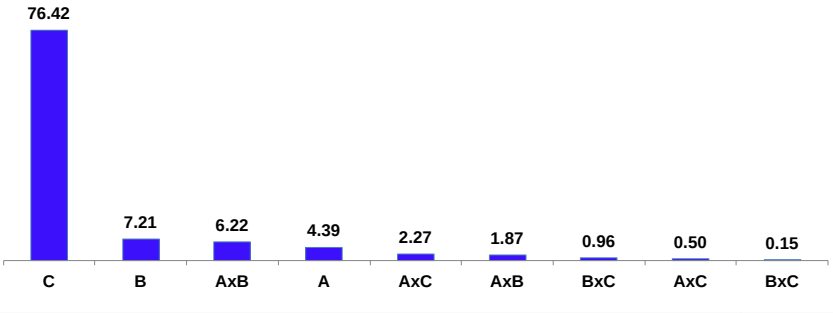								
Cumulative contribution	76.42	83.63	89.85	94.24	96.51	98.38	99.35	99.85	100.00
Check on significant interaction			AXB two-way table						
Optimum combination of significant factor level			A2B2C0						

The response table and response graphs of the mean S/N ratio are presented in Table 10 and shown in Fig. 5, respectively. The results confirm the findings of the Pareto ANOVA analysis, summarized in Table 9. Table 10 and Figure 5 show that parameter C (feed rate) has the most significant effect on surface roughness, and its low level (C0) produced the best surface roughness. For selecting the best combination of parameters A and B, a two-way table of A × B interactions was applied. The table showed that A2B2 yielded the best surface roughness. Therefore, the combination of input parameters for achieving the best surface roughness is A2B2C0 i.e., square-shaped insert (nose angle of 80°), high level of nose radius (1.2 mm), and low level of feed rate (0.11 mm/rev).

Table 10: Response table of mean S/N ratio for surface roughness, and significant interaction

		Mean S/N Ratio			
Input Parameters	**Symbol**	**Level 0**	**Level 1**	**Level 2**	**Max - Min**
Insert Shape	A	-6.75	-5.23	-2.85	3.90
Noise Radius	B	-7.82	-3.89	-3.12	4.70
Feed Rate	C	3.52	-5.51	-12.85	16.37
Interaction A×B	B×C	-2.38	-6.96	-5.50	4.58

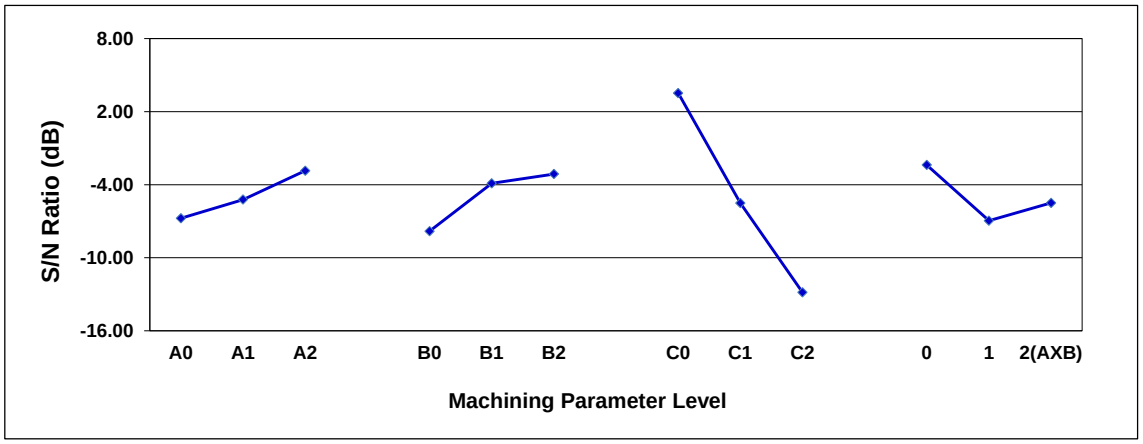

Fig. 5 Response graphs of mean and S/N ratio for surface finish

The results of traditional analyses, showing the averaged variation of surface roughness values for three input parameters, are presented in Fig. 6. The dominant effect of feed rate is evident from this figure. Moreover, the figure shows that the best surface roughness is achieved by using a square-shaped insert (nose angle of 80°), high level of nose radius (1.2 mm), and low level of feed rate (0.11 mm/rev). These findings confirm those obtained from the Pareto ANOVA analysis, given in Table 9, and the Taguchi method, summarized in Table 10 and shown in Fig. 6.

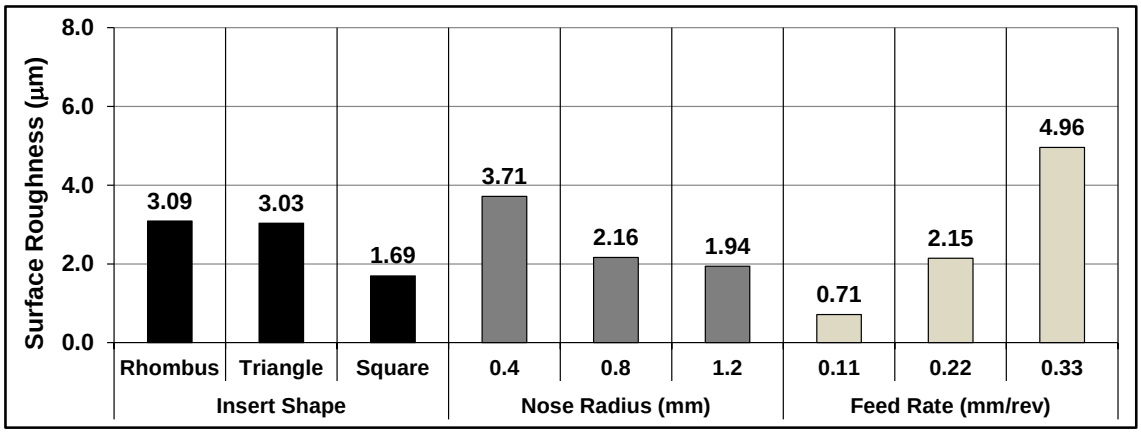

Fig. 6 Average variation of surface finish for three input parameters

5. DISCUSSION

The results and subsequent analyses presented above show that the two selected tool geometry parameters—insert shape and nose radius—have a considerable effect on diameter error and minor effects on circularity and surface finish. The major contributor to surface finish is feed rate, whereas circularity is dominated by interaction effects.

The most influential parameter for diameter error is nose radius (Table 5). The higher the nose radius, the lower is the peak-to-valley height of the turned surface, thus resulting in a more uniform surface profile. As a result, material removal is increased along the normal to the cutting direction, and material removal is more accurate. However, nose radius effectiveness depends on the feed rate. Although the diameter error increases with an increase in the feed rate, the individual effect of feed rate is minor (3.72% contribution). At a nose radius of 0.8 mm for the variables considered in this investigation, the interaction of feed rate and nose radius is seemingly unfavorable from the viewpoint of dimensional accuracy.

Diameter error, too, is influenced by nose angle (Table 5). Figures 1 and 2 show that initially, as the nose angle increased, diameter error improved slightly. However with

further increase in nose angle, diameter error deteriorated. The most likely cause of the increase in diameter error is elastic deformation of the workpiece, which increases with increased cutting force resulting from the increase in nose angle. In contrast, although the nose angle of the rhombus-shaped insert is small, its overhang is longer than those of other inserts. This may induce elastic deformation in the insert.

Table 7 shows that the circularity error is dominated by interaction effects. Insert shape (nose angle) and nose radius have minor effects on circularity (1.03% and 2.64% contribution, respectively). Rafai and Islam [17] stated that the primary cause of circularity error is radial cutting force. With an increase in nose radius, radial cutting force increases [22], resulting in increased circularity error (Figures 3 and 4).

The most influential parameter for surface roughness is feed rate, followed by nose radius (Table 9). The results show clear trends, which are expected, and conform to the relationship expressed by Eq. (1). Although the influence of insert shape is on surface roughness is negligible (4.39% contribution), the influence of insert shape showed a clear trend. Surface roughness values decrease as nose angle increases owing to a decrease in the peak-to-valley height caused by a larger nose angle. The square-shaped insert, which has the largest nose angle, generated the best surface finish.

6. CONCLUSION

This investigation considered three important parameters—insert shape (nose angle), nose radius, and feed rate on three quality characteristics of turned parts—dimensional error, circularity, and roughness. From the experimental results and subsequent analyses, the following conclusions can be drawn:

- Two of the selected insert geometry parameters—insert shape and nose radius—have considerable effects on diameter error (16.92% and 50.05% contributions, respectively). It seems that the variation of elastic deformation of the workpiece and cutting tool owing to the variation of these two parameters causes the diameter error. The effects of interactions among different parameters are relatively minor in this case.
- Circularity is dominated by interaction effects, with the interaction between insert shape and feed rate being the major contributor (31.44% contribution). The two selected insert geometry parameters—insert shape and nose radius—showed negligible effects (1.03% and 2.64% contributions, respectively).

- The main contributing factor to surface roughness is feed rate (76.42% contribution). The two selected insert geometry parameters—insert shape and nose radius—have minor effects on surface roughness (4.39% and 7.21% contributions, respectively). With an increase in insert nose angle and/or nose radius, surface roughness improved, whereas with an increase in feed rate, surface roughness deteriorated.

ACKNOWLEDGEMENT

The authors would like to acknowledge the contribution of Mr. B. G. M. Gharh, a Master of Engineering student at the Department of Mechanical Engineering, Curtin University, Australia.

REFERENCES

[1] Drozda, T.J. &Wick, C. (1983) Tool and Manufacturing Engineers Handbook, Volume 1, Machining. SME, Dearborn.

[2] Fang, N., & Wu, Q. (2005). The effects of chamfered and honed tool edge geometry in machining of three aluminum alloys. *International Journal of Machine Tools and Manufacture*, 45(10), 1178-1187.

[3] Almeida, F. A., Oliveira, F. J., Sousa, M., Fernandes, A. J. S., Sacramento, J., & Silva, R. F. (2005). Machining hardmetal with CVD diamond direct coated ceramic tools: effect of tool edge geometry. *Diamond and related materials*, 14(3), 651-656.

[4] Özel, T., & Zeren, E. (2007). Finite element modeling the influence of edge roundness on the stress and temperature fields induced by high-speed machining. *The International Journal of Advanced Manufacturing Technology*, *35*(3-4), 255-267.

[5] Thiele, J. D., & N Melkote, S. (1999). Effect of cutting edge geometry and workpiece hardness on surface generation in the finish hard turning of AISI 52100 steel. *Journal of Materials Processing Technology*, 94(2), 216-226

[6] Hua, J., Shivpuri, R., Cheng, X., Bedekar, V., Matsumoto, Y., Hashimoto, F., & Watkins, T. R. (2005). Effect of feed rate, workpiece hardness and cutting edge on subsurface residual stress in the hard turning of bearing steel using chamfer+ hone cutting edge geometry. *Materials Science and Engineering: A*, 394(1), 238-248.

[7] Nomani, J., Pramanik, A., Hilditch, T., & Littlefair, G. (2013). Machinability study of first generation duplex (2205), second generation duplex (2507) and austenite stainless steel during drilling process. *Wear*.

[8] Günay, M., Aslan, E., Korkut, I., & Seker, U. (2004). Investigation of the effect of rake angle on main cutting force. *International Journal of Machine Tools and Manufacture*, *44*(9), 953-959.

[9] Liu, M., Takagi, J. I., & Tsukuda, A. (2004). Effect of tool nose radius and tool wear on residual stress distribution in hard turning of bearing steel. *Journal of Materials Processing Technology*, *150*(3), 234-241.

[10] Usui, E., & Hirota, A. (1978). Analytical Prediction of Three Dimensional Cutting Process—Part 2: Chip Formation and Cutting Force with Conventional Single-Point Tool. *Journal of Engineering for Industry*, *100*, 229.

[11] Lo, S. P. (2000). An analysis of cutting under different rake angles using the finite element method. *Journal of materials processing technology*, *105*(1), 143-151.

[12] Saglam, H., Unsacar, F., & Yaldiz, S. (2006). Investigation of the effect of rake angle and approaching angle on main cutting force and tool tip temperature. *International Journal of Machine Tools and Manufacture*, 46(2), 132-141.

[13] Pramanik, A., Neo, K. S., Rahman, M., Li, X. P., Sawa, M., & Maeda, Y. (2008). Ultra-precision turning of electroless-nickel: Effect of phosphorus contents, depth-of-cut and rake angle. *Journal of Materials Processing Technology*, 208(1), 400-408.

[14] Dogra, M., Sharmab, V. S., & Durejac, J. (2011). Effect of tool geometry variation on finish turning–A Review. *Journal of Engineering Science and Technology Review*, *4*(1), 1-13.

[15] Marcos-Bárcena, M., Sebastián-Pérez, M. A., Contreras-Samper, J. P., Sánchez-Carrilero, M., Sánchez-López, M., & Sánchez-Sola, J. M. (2005). Study of roundness on cylindrical bars turned of aluminium–copper alloys UNS A92024. *Journal of Materials Processing Technology*, 162, 644-648.

[16] Tzeng, C. J., Lin, Y. H., Yang, Y. K., & Jeng, M. C. (2009). Optimization of turning operations with multiple performance characteristics using the Taguchi method and Grey relational analysis. *Journal of materials processing technology*, *209*(6), 2753-2759.

[17] Rafai, N. H., & Islam, M. N. (2009). An investigation into dimensional accuracy and surface finish achievable in dry turning. *Machining Science and Technology*, 13(4), 571-589.

[18] Dhar, N.R.; Islam, M.W; Islam, S.; Mithu, M.A.H. (2006) The influence of minimum quality lubrication (MQL) on cutting temperature, chip and dimensional accuracy in turning AISI-1040 steel, *Journal of Materials Processing Technology*, 171: 93-99.

[19] Dhar, N. R., S. Paul, and A. B. Chattopadhyay (2001) The influence of cryogenic cooling on tool wear, dimensional accuracy and surface finish in turning AISI 1040 and E4340C steels. *Wear*, 249(10), 932-942.

[20] Islam, M. N. (2013). Effect of additional factors on dimensional accuracy and surface finish of turned parts. *Machining Science and Technology*, 17(1), 145-162.

[21] Kalpajian, S. Schmid, S.R. (2010) Manufacturing Engineering and Technology, sixth ed., Pearson Education Inc., New Jersty.

[22] Insert nose radius, Sandnik webpage, http://www.sandvik.coromant.com/en-gb/knowledge/general_turning/how-to-achieve-good-component-quality/insert-information/insert-nose-radius/pages/default.aspx Accessed 10 June 2014.

[23] Armarego, E.J.A., & Brown, R.H. (1969) The Machining of Metals, Prentice Hall, Inc., New Jersey.
[24] Park, S.H. (1996) Robust Design and Analysis for Quality Engineering, Chapman & Hall, London
[25] Ross, P.J. (1988) Taguchi Techniques for Quality Engineering, McGraw-Hill, New York.
[26] Insert Nomenclature - Home Model Engine Machinist, http://www.google.com.au/url?url=http://www.homemodelenginemachinist.com/attachments/f13/59299d1356359417-what-size-triangular-inserts-insertnomenclature.pdf&rct=j&frm=1&q=&esrc=s&sa=U&ei=V7CXU6SGHoeYkQX1w4GwCw&ved=0CBQQFjAA&sig2=Dkt-zWMjD-KmPHvAyHIXdw&usg=AFQjCNFcH_vAMA1OyBwW6iCKI-j0J7x9Zg Accessed 10 June 2014.
[27] Taguchi,G. (1987) System of Experimental Design: Engineering Methods to Optimize Quality and Minimize Cost, Vol. 2, UNIPUB/Kraus Int. Pub., White Plains, NY.
[28] MatWeb, *Material Property Data*, http://www.matweb.com/ Accessed 10 June 2014.